

High power injection seeded optical parametric oscillator

D.C. Hovde, J.H. Timmermans, G. Scoles and K.K. Lehmann

Department of Chemistry, Princeton University, Princeton, USA

Received 14 May 1991; revised manuscript received 29 July 1991

We have demonstrated the feasibility of an infrared optical parametric oscillator (OPO) without frequency control elements that produces near transform limited 120 MHz bandwidth, 10 ns pulses via injection seeding. The experimental threshold for injection seeding at 1.5 μm is only a few μW , and the OPO cavity is easily locked to the seed laser. Using a poor spatial quality 540 Hz YAG laser as a pump source, we have obtained 1.5 μm pulse energies of 3 mJ/pulse ($> 10\%$ energy conversion). However, at present, the OPO gain falls below threshold after continuous operation for ~ 1 hour, due to reversible degradation of the LiNbO_3 crystal. A small frequency shift between seed and output frequencies is observed and possible mechanisms are discussed.

1. Introduction

Intense, tunable, narrow spectral bandwidth infrared pulses are essential for a new generation of experiments in molecular and cluster dynamics and spectroscopy, nonlinear optics, surface sum frequency generation, remote sensing, and multiphoton photodissociation. Efficiency and signal/noise typically scale with the repetition rate, so many experiments can be performed only with a high average power system. Advances in the spatial mode quality and average power of pulsed solid state lasers should now make it possible to pump an optical parametric oscillator (OPO) at high repetition rate and high average power, while preserving the broad tunability and excellent energy conversion efficiency demonstrated at low repetition rate. Herein we describe our efforts to develop a 100 kW peak power, 1 W average power tunable infrared source with 100 MHz (or 0.003 cm^{-1}) spectral bandwidth.

Two methods have been used to obtain single mode (SM) output from pulsed, high power OPOs. Wavelength selective elements can be added to the cavity to suppress the gain on all but a single mode [2,5,6,7] or radiation can be injected into the cavity to selectively enhance the build up of a single mode [8–11]. Minton et al. [7] recently demonstrated a tunable infrared SM OPO using a combination of beam expanding prisms, grating and etalon. When pumped

near threshold, their OPO could be scanned under computer control over 90 GHz intervals with frequency resolution of about 200 MHz in the unresonated wave.

The first SM OPO was demonstrated by Bjorkholm and Danielmeyer [8], who seeded a cw single mode Nd:YAG laser into a ruby laser pumped LiNbO_3 OPO to reduce the output bandwidth. In their demonstration, no tuning of the seed wavelength was possible. Injection seeding also lowers the oscillation threshold and improves energy conversion efficiency [9,10,12]. To control the bandwidth in our work we have chosen to use injection seeding because this method will offset the expected reduced gain caused by the poorer mode quality of a high average power pump laser. Seeding requires an external laser of modest power (a few μW) and good spectral properties. Today these requirements can be met routinely with commercial infrared diode lasers or color center lasers. The seed laser also serves as a probe of the OPO dynamics, as we discuss below.

In this paper we demonstrate a practical device for producing intense, tunable, near transform limited pulses of infrared radiation: an injection seeded LiNbO_3 optical parametric oscillator. When pumped by 22 mJ, 15 ns pulses from a single longitudinal mode, 540 Hz repetition rate Nd:YAG laser and seeded by 20 mW from a cw single mode 1.5 μm color center laser, the OPO produces near transform lim-

ited 3 mJ signal wave pulses of 10 ns duration and 120 MHz spectral bandwidth. The resonated signal wave is continuously tunable across the range 1.47–1.68 μm (limited at present by the dichroic reflector used to couple in Nd:YAG radiation to the cavity). The unresonated idler range is 2.90–3.85 μm . In preliminary experiments, the bandwidth of the idler wave was measured with a confocal etalon to be 450 mHz. The narrow idler bandwidth follows from energy conservation and the use of a narrow bandwidth pump laser.

Although single mode operation of the OPO is routinely obtained, we emphasize that the signal wave output is not phase-locked to the seed laser. At such high gain, the capture range for locking is very narrow, requiring that a cavity mode coincides with the seed frequency to within about 100 kHz. The cavity was actively stabilized for maximum transmission of the seed laser with an estimated accuracy of 20 MHz. By analogy to laser seeding, we expected the output to occur at the frequency of the OPO cavity mode nearest the seed frequency [13]. Instead we observed that the signal wave output was shifted 80 MHz from the seed frequency. Possible mechanisms for this shift that we are investigating include cavity pulling due to the nonlinear index of refraction in the presence of the strong pump field, frequency pulling by unwanted idler feedback or phase mismatch.

2. Experimental

The injection seeded OPO consists of the LiNbO_3 crystal in a folded 7 cm long cavity resonant at 1.5 μm , an injection seeded 1.06 μm Nd:YAG pump laser, and a computer controlled single mode, cw 1.5 μm color center seed laser pumped by a cw mode-locked Nd:YAG laser. Fig. 1 shows the experimental layout.

The flashlamp pumped, electro-optically Q-switched Nd:YAG laser oscillator and amplifiers (Quantel YG500 QS) produce 100 mJ, 15 ns pulses at 1.064 μm with spatial mode quality and polarization showing the effects of the large thermal load on the Nd:YAG rods [14]. A commercial cw seed laser (lightwave) produces smooth temporal mode quality, with a specified bandwidth of 120 MHz. The

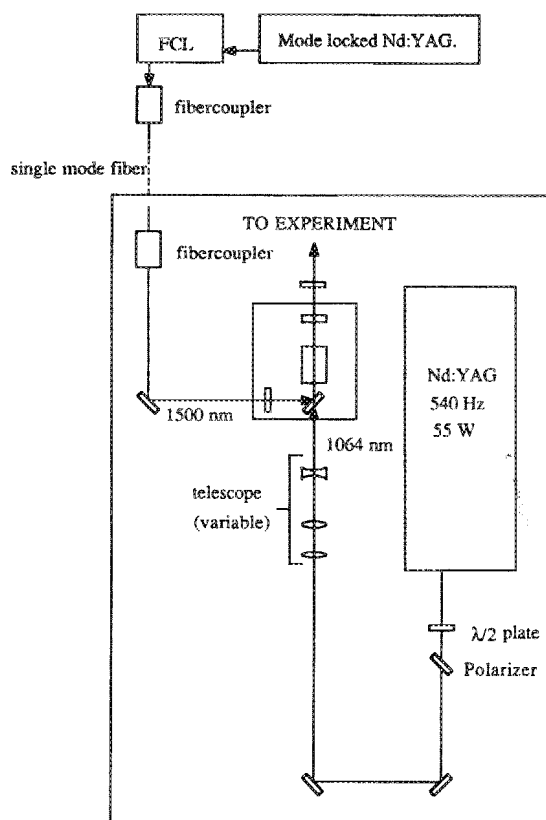


Fig. 1. Layout of the experimental set-up of the OPO. The half wave plate in combination with the polarizer allows us to vary the power incident on the crystal. With the telescope, we control the spot size.

power oscillator cavity length is servo locked by dithering the end mirror and minimizing the output pulse build up time. This locking scheme causes 10 MHz pulse to pulse changes in the frequency of the pump laser and, by energy conservation, in the idler output. Escherich and Owyong [15] have shown that the seed laser can be locked to the power oscillator without frequency dithering. The strong temperature dependence of the seed laser frequency (3 GHz K^{-1}) may cause long term frequency shifts despite temperature stabilization of the seeder. We plan to measure the Nd:YAG seed wavelength with a travelling wavemeter.

In the experiments performed so far, the output energy has been reduced to 22 mJ by delaying the firing of the flashlamps that pump the final amplifier, in order to reduce the power load on the LiNbO_3

crystal. At full power (35 W, 65 mJ/pulse), the crystal temperature rose 25°C during operation, and successful seeding was not observed.

The pump laser is propagated 6 m, then imaged onto the OPO cavity by a zoom telescope consisting of three plano-curved AR coated fused silica lenses which are adjusted to collimate the beam horizontally; the slightly elliptical beam weakly diverges vertically due to thermal astigmatism introduced in the amplifiers. The peak fluence is 1.5 J/cm² and the peak power is 100 MW/cm².

Radiation from a 1.5 µm color center laser operated in cw mode (Burleigh FCL 120), pumped with the 1.8 W output from a cw mode locked Nd:YAG laser (Spectra Physics 3460), seeds the OPO. After picking off beams for a 7.5 GHz etalon and a reference gas cell, the main beam (up to 180 mW) is directed through a Faraday isolator into a single mode fiber (8.5 µm fused silica core, 125 µm doped silica cladding, loss of 4 dB/km). (A polarization preserving fiber would be better for this application.) The fiber delivers the seed beam to an adjacent lab that contains the Nd:YAG laser and OPO apparatus, where a 5× microscope objective softly focuses the seed beam to a spot size of about 1 mm at the OPO input coupler 1 m away. The entire fiber output coupling assembly is mounted on an *x-y* translation stage so that the seed and signal beams can be overlapped. Losses in the Faraday isolator and in the fiber couplers reduce the power incident on the OPO input coupler to 20 mW (polarization scrambled).

The L-shaped OPO cavity consists of three 25.4 mm diameter dielectric mirrors and the LiNbO₃ crystal (10×10×50 mm, Crystal Technologies); no frequency selective elements are used. The three cavity mirrors are the input coupler (commercial diode laser input coupler 95% *R* at 1.55 µm), the YAG input coupler (custom dichroic – high *R* at 1.5 µm s-polarized, high *T* at 1.06 µm p-polarized), and the output coupler (custom 50% *R* at 1.5 µm, <15% at 1.06 and 3.5 µm, CaF₂ substrate). A piezoelectric translator (PZT) supports the input coupler so that cavity modes can be matched to the seed frequency. The mounts for the three optical components are screwed top and bottom onto two soft iron plates. The crystal is held in a brass oven stabilized near 35°C; the oven is mounted on a rotation stage that has an accuracy of 6 arc s.

A standard 1.06 µm high reflector mirror placed immediately after the output coupler has proven satisfactory for separating the signal output from the pump. The substrate absorbs strongly in most of the idler region 2.5–4 µm, but near 3.3 µm it transmits 30%, so that characterization of the idler output was done at this wavelength.

The OPO cavity is locked to the maximum transmission of the ordinary 1.5 µm seed ray using standard servo techniques, with the following two precautions. To eliminate frequency jitter of the signal wave imposed by modulating the cavity length, the modulation applied to the PZT is phaselocked to the fifth harmonic of the pump laser repetition frequency. This ensures that the Nd:YAG laser fires always at the same point in the modulation cycle, and permits us to lock the low finesse cavity with a length modulation corresponding to a large (200 MHz pp) frequency excursion. We estimate the locking error is less than 20 MHz. To observe the relatively weak seed laser, we have found it necessary to discriminate against the much higher power signal beam. Because the pump laser fires at the harmonic of the line frequency, a chopper wheel driven by a line synchronous motor is able to block the signal wave from reaching the seed laser detector. The chopper blade is cut to block a full modulation cycle so that to first order the servo loop is unaffected.

3. Results

Operating the pump laser while delaying the flashlamps for the final amplifier reduces the Nd:YAG output power to 12 W after the linear polarizer. The OPO then produces up to 1.5 W of signal wave radiation when injection seeded versus 0.75 W unseeded. The energy conversion efficiency thus exceeds 10% for the seeded OPO. Initially, the output power is stable to within 10% on short time scales. After several hours of operation, the power drops by 50% and becomes very unstable. This appears to result from reversible photorefractive degradation of the LiNbO₃ crystal. In its present design, the crystal oven is incapable of operating above 70°C without introducing unacceptable temperature gradients. Operating above 150°C should allow photorefractive damage to relax between pulses, thus permitting

long term operation at maximum efficiency.

Using a 10 Hz repetition rate laser, we characterized the range of conditions over which seeding was successful. Using 20 mW unpolarized light at 1.524 μm , seeding improved the output power over an external angle range ± 0.6 mrad, and a wavelength range ± 1 nm. Both measurements correspond to a phasematching tolerance $\text{sinc}^2(\Delta k L/2) = 0.5$. The OPO could be seeded with as little as 1.5 μW incident on the input coupler. Experience with the high rep rate pump laser system shows qualitatively similar behavior. Etalon transmission spectra were used to characterize the spectral properties of the signal beam (using the high rep rate pump laser system) and the idler (using the 10 Hz system). The signal wave at 1.5 μm was examined with a 60 GHz etalon. Fringes were not observed for the unseeded OPO, indicating that the linewidth for the unseeded OPO exceeded that measured by Brosnan and Byer [2], 66 GHz, under similar experimental conditions. The seeded OPO appeared only slightly broader than the instrument resolution (1.2 GHz versus 0.9 GHz). A 750 MHz etalon with a resolution of 30 MHz gave a definitive measurement of the signal wave linewidth: 120 MHz fwhm (fig. 2). Additional frequency jitter of about 50 MHz was observed on an oscilloscope, with a time scale of a few seconds. The observed time bandwidth product is consistent with a frequency chirp of 11 MHz/ns. With the low rep rate laser, the linewidth of the idler was measured with an etalon of resolution 150 MHz to be ≤ 450 MHz. (In this low rep rate case the signal wave bandwidth was 180 MHz due to the shorter duration of the pump pulse.)

The signal wave was also used to excite the photoacoustic spectrum of several overtone transitions of acetylene at 1.52 μm . However, the room temperature Doppler broadening of the transitions precluded their use for measuring the OPO spectral linewidth. Both the etalon traces and the acetylene spectra indicated a systematic shift of the signal wave 80 MHz lower in frequency relative to the seed laser.

The signal wave was measured with a fast piezoelectric detector directly mounted on a digitizing oscilloscope. The measured 9.5 ns fwhm pulse width agreed well with the estimate from the depletion of the pump laser observed with a fast photodiode (10 ns).

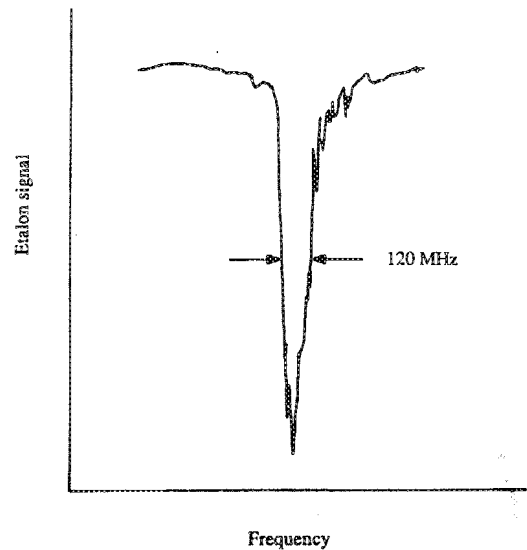


Fig. 2. 750 MHz etalon trace of the signal wave showing a signal linewidth of 120 MHz fwhm.

4. Theory of injection seeded OPOs

The theory of the pulsed OPO is well understood [1,2,16,17]. Here we review those aspects of the theory needed to explain the increased power conversion efficiency and dramatically reduced linewidth that result from injection seeding, and the effects of unwanted idler feedback. In the presence of an intense "pump" field at frequency ω_p , a medium having a second order nonlinear polarizability will exhibit gain at pairs of frequencies ω_s ("signal wave") and ω_i ("idler"). The coupled field equations have an analytic solution for the early "build up" phase of the oscillator when pump depletion can be neglected. The signal field at the output end of the crystal is constructed from three phasors: simple gain at 0° , a phase mismatched term at $\pm 90^\circ$, and gain due to an idler input, with phase angle determined by the idler phase relative to the signal and pump [16,17]:

$$\begin{aligned}
 A_s(L) \exp(i\Delta k L/2) \\
 = A_s(0) \left[\cosh(bL) - \frac{i\Delta k}{2b} \sinh(bL) \right] \\
 - \frac{i\Gamma}{2b} A_i^*(0) \sinh(bL), \quad (1)
 \end{aligned}$$

where b is the effective gain coefficient including phase mismatch,

$$b = \frac{1}{2}i[\Gamma^2 - (\Delta k^2)]^{1/2}.$$

The phase mismatch $\Delta k = k_p - k_s - k_i$, is a strong function of propagation angle and temperature. Γ is proportional to the electric field of the pump radiation and to the d_{eff} coefficient of the nonlinear material (see ref. [16]). L is the coherent interaction length within the crystal. Eq. (1) predicts that the small signal power gain reaches 2×10^6 per pass in our experiments.

Because the gain decays instantly on the nanosecond timescale, the efficiency of pulsed OPOs is limited by the number of round trips that allow the resonated wave to build up during the pump pulse. Brosnan and Byer have developed a model for the coherent gain needed for a singly resonant OPO to reach threshold that makes explicit the effects of the build-up time [2], which can be simplified under our experimental conditions:

$$\Gamma L = (t_c/\tau) \ln(P_{\text{thr}}/P_0) + 2aL - \frac{1}{2} \ln R + \ln 2. \quad (2)$$

The pump pulse duration is τ , the cavity round trip time is t_c , and the output coupling mirror has reflectivity R . P_{thr} is the threshold power level. P_0 is the initial power level at time $t=0$; for the unseeded OPO, the initial distribution is due to vacuum fluctuations of the quantized field. The OPO is seeded by increasing P_0 for a single cavity mode by injecting radiation from a low power single mode laser. Due to its smaller ratio P_{thr}/P_0 the seeded mode threshold is lowered and it can begin to deplete the pump while the other modes still contain little power [8]. Assuming equal gain for the seeded mode and N competing modes gives an estimate for the minimum seed power $P_s \gg NP_n$, where P_n is the circulating noise power per cavity mode, about 100 pW. For our cavity and assuming a 10 cm^{-1} gain bandwidth, $N=250$ so that $P_0 \gg 25 \text{ nW}$ for seeding to be successful.

Once the pulse enters the pump-depleted regime, the signal wave power approaches steady state. If the seeded mode is not exactly at the peak of the phase matched gain curve, unseeded modes with greater gain will continue to grow, although more slowly than when the pump was undepleted. At long times, the mode with the highest gain will overtake the seeded

mode [8]. OPOs with longer pump pulses require seeding closer to the peak of the gain curve. Numerical calculations for a gaussian pump pulse [18] indicate that seeding is successful for 35 ns pulses if $\text{sinc}^2(\Delta k L/2) \geq 0.8$. Bjorkholm and Danielmeyer [8] demonstrated seeding over the duration of a 10 ns output. We observe increased power from seeding if $\text{sinc}^2(\Delta k L/2) \geq 0.5$.

We next consider mechanisms that affect the phase of the signal wave in a pulsed OPO. From eq. (1), the phase of the output is modified by imperfect phasematching. For small phase mismatch (within the undepleted pump approximation!), the shift $\Delta\phi_s$ is

$$\Delta\phi_s(\Delta k) = (\Delta k/2b) \tanh(bL) - \Delta k L/2. \quad (3)$$

As the effective gain b goes to infinity, this term approaches $-\Delta k L/2$, reaching half this limiting value when $bL=1.92$. The highest value of bL attained in our experiments is 7.9. The phase shift per round trip is equivalent to a frequency shift, $\Delta f = \delta\Phi/\Delta t$, of the signal output [13]. Eq. (3) predicts an 80 MHz shift for a phase mismatch $\Delta k L = 0.16$ or about 6% of the observed seeding range, for the largest laser field. Because it varies somewhat with pump intensity, the phase mismatch term will also contribute to a frequency chirp.

Eq. (1) also predicts that the signal phase will be modified by an idler input. Although the initial idler noise field can be neglected in comparison to the injection seeded field (it causes a transient phase shift [1,19]), unwanted feedback of the amplified idler wave results in an input $A_i = (r_i/r_s)A_s$ [20,21], where r is the net complex field coefficient that describes the phase and amplitude to propagate from the output of the crystal back to the input face. Assuming a monochromatic pump wave, the result is a phase shift

$$\Delta\phi_s(\text{feedback}) = (r_i/r_s) \tanh(bL), \quad (4)$$

which reaches half its limiting value when $bL=0.55$. Power feedback of 2% ($|r|=0.14$) can produce an 80 MHz frequency shift. This mechanism is not likely to produce a frequency chirp, since the phase shift saturates at 10% of the full pump power. The effects of idler feedback are probably more pronounced when using a narrow bandwidth pump laser, such as our injection seeded Nd:YAG laser. A broadband

pump laser will excite many idler frequencies, which differ in the phase angles of the r_i (r_s is servo locked to the seed laser). The net phase shift to the signal wave will represent a dynamic average over these modes, weighted most heavily toward the idler modes that grow fastest, i.e., those that are nearly doubly resonant. The bandwidth of a multimode Nd:YAG laser, 0.7 cm^{-1} , would excite idler modes with a spread of 270° in the phase of r_i . To avoid crystal damage, we did not attempt to pump the OPO with multimode radiation, so this proposition remains untested.

Finally we note that the signal wave cavity resonance frequency, $c/2(nL+L')$, is modified by the intense pump field through the nonlinear index of refraction

$$n = n_0 + n_2 \langle E^2 \rangle + \dots \quad (5)$$

This will also modify the output of the signal wave. Although an accurate measurement of n_2 is not available for this important material, an estimate can be made using the empirical relations of Adair et al. [22]. This gives $n_2 = 4 \times 10^{-12}$ esu, resulting in a frequency shift of 30 MHz at the highest fields in our study. Because the nonlinear index follows the pump profile, this mechanism will chirp the frequency of the signal wave.

In fig. 3, we show the dependence of the three phase shift mechanisms as a function of bL . All three were adjusted to give the same phase shift at $bL = 7.9$, which is the highest gain in our experiment.

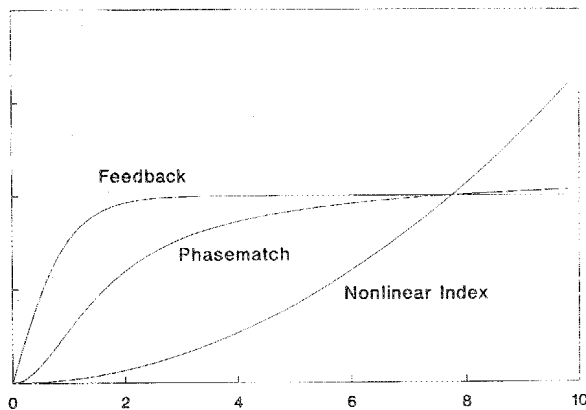


Fig. 3. Dependence of the three phaseshift mechanisms discussed as a function of gain. Parameters were chosen so that the curves intersect at the highest value of bL attained in our experiments.

5. Conclusions

We have demonstrated the feasibility of LiNbO₃ OPOs at high average power and high repetition rate. Energy conversion efficiency doubles and spectral bandwidth is reduced to a single mode, by injection seeding with 20 mW from a stable cw oscillator. The pulse-duration-bandwidth product $10 \text{ ns} \times 120 \text{ MHz} = 1.2$ is very close to the Fourier limit of a gaussian pulse (0.44), indicating little amplitude or phase substructure in the pulse. Photorefraction degrades reversibly the performance of LiNbO₃ at high rep rate, and will require the use of other materials, or operation at high temperatures. Phasematching errors, feedback of the unresonated idler and second order index effects act to shift and chirp the OPO output; these effects must be considered for high resolution work.

Acknowledgements

The authors would like to thank professor Robert Byer for useful discussions. Also, we gratefully acknowledge the financial support of the Army Research Office, Princeton POEM, the Henry and Camille Dreyfuss Foundation, and the National Science Foundation.

References

- [1] R.A. Baumgartner and R.L. Byer, IEEE J. Quantum Electron. 15 (1979) 433.
- [2] S.J. Brosnan and R.L. Byer, IEEE J. Quantum Electron. 15 (1979) 415.
- [3] R.L. Byer, R.L. Herbst and R.N. Fleming, in: Laser spectroscopy, eds. S. Haroche et al. (Springer, Berlin, 1975).
- [4] K. Kato, IEEE J. Quantum Electron. 16 (1980) 1017.
- [5] L.B. Kreuzer, Appl. Phys. Lett. 15 (1969) 263.
- [6] J. Pinard and J.F. Young, Optics Comm. 4 (1972) 425.
- [7] T.K. Minton, S.A. Reid, H.L. Kim and J.D. McDonald, Optics Comm. 69 (1989) 289.
- [8] J.E. Bjorkholm and H.G. Danielmeyer, Appl. Phys. Lett. 15 (1969) 171.
- [9] I. Ya Itskhoki and S.L. Seregin, Sov. J. Quant. Electron. 10 (1980) 515.
- [10] U.A. Abdullin, G.P. Dahotyan, Y.E. D'yakov, B.V. Zhdanov, V.I. Pryalkin, V.B. Sobolev and A.I. Kholodnykh, Sov. J. Quant. Electron. 14 (1984) 538.

- [11] Y.X. Fan, R.C. Eckardt, R.L. Byer, J. Nolting and R. Wallenstein, *Appl. Phys. Lett.* 53 (1988) 2014.
- [12] A.G. Marunkov, V.I. Pryalkin and A.I. Kholodnykh, *Sov. J. Quantum Electron.* 11 (1981) 869.
- [13] A. Siegman, *Lasers* (University Science Books, Mill Valley CA, 1986), chapter 29.
- [14] Koechner, *Solid state laser engineering* (Springer, Berlin, 1976) chapter 7.
- [15] P. Esherick and A. Owyong, *J. Opt. Soc. Am. B* 4 (1987) 41.
- [16] A. Yariv, *Quantum electronics*, 2nd Ed. (Wiley, New York, 1975), chapter 17.
- [17] R.G. Smith, *J. Appl. Phys.* 41 (1970) 4121.
- [18] E.S. Cassedy and M. Jain, *IEEE J. Quantum Electron.* 15 (1979) 1290.
- [19] K.C. Rustagi, S.C. Mehendale and S. Meenakshi, *IEEE J. Quantum Electron.* 18 (1982) 146.
- [20] J. Falk, *IEEE J. Quantum Electron.* 7 (1971) 230.
- [21] R.C. Eckhardt, C.D. Nabors, W.J. Kozlowsky and R.L. Byer, *J. Opt. Soc. Am. B* 8 (1991) 646.
- [22] R. Adair, L.L. Chase and S.A. Payne, *Phys. Rev. B* 39 (1989) 3337.